Biomechanics of static roll posture control by body flexion in adult zebrafish

Ryota Nagaoka[1,2,3], Taisei Katayama[1,2,4], Shin-ichi Higashijima[1,2,3], Masashi Tanimoto[1,2,3,5,*]

[1]Division of Behavioral Neurobiology, National Institute for Basic Biology, Okazaki, Aichi 444-8787, Japan

[2]Neuronal Networks Research Group, Exploratory Research Center on Life and Living Systems, Okazaki, Aichi 444-8787, Japan

[3]The Graduate University for Advanced Studies, SOKENDAI, Okazaki, Aichi 444-8787, Japan

[4]Division of Biological Science, Graduate School of Science, Nagoya University, Nagoya, Aichi 464-8602, Japan

[5]Lead contact

[*]Correspondence: tanimoto@nibb.ac.jp

Summary

Posture control is crucial for animals. Static posture control in fish remains poorly explored. Recent studies have shown that larval zebrafish perform body flexion during slight roll tilts: the body flexion displaces a gas-filled swim bladder, generating counter-rotation torque for postural recovery through misalignment of gravity and buoyancy forces. Swim bladder deflation impairs this postural recovery, suggesting its critical role. This static posture control strategy may be utilized by many fish species. However, adult fish differ from larvae in morphology and behavior, raising questions about the generality of this mechanism. Our behavioral analysis showed that adult zebrafish also flexed their body during roll tilts, with flexion persisting until recovery to an upright posture. Similarly to larvae, swim bladder deflation impaired postural recovery. These results demonstrate that adult fish employ static roll posture control through body flexion and suggest the generality of this mechanism in fish species.

Introduction

For many animals, posture control is crucial for survival, regardless of whether they live on the land or in the water. Terrestrial animals use both dynamic and static postural control mechanisms.[1–3] When posture is significantly disrupted, animals dynamically move their limb and axial muscles to recover their desired posture. Even during seemingly motionless periods, static postural control through anti-gravity muscle tone continuously maintains posture.

How about postural control in fish? Previous studies have been predominantly centered on dynamic movements involving swimming and fin dynamics.[4–8] In contrast, our understanding of static postural control mechanisms remains limited. This is particularly intriguing because most fish species are inherently unstable[7] - anesthetized or dead fish typically roll to a belly-up position due to their mass distribution.[6,9–11] Nevertheless, many fish species maintain an upright posture even while appearing motionless.[9,10] These common observations suggest the existence of static postural control mechanisms through neuromuscular activity. However, until recently, the underlying mechanisms of this static postural control remained poorly understood.

Recent studies on millimeter-sized larval zebrafish have provided valuable insights into this longstanding question. When slightly roll tilted or artificial vestibular stimulation mimicking a head roll tilt was applied, larval zebrafish perform body flexion and recover an upright posture.[12–16] This body flexion behavior is driven by neural circuits, from a vestibular nucleus via reticulospinal neurons projecting to the spinal cord, and the posterior hypaxial muscles (PHM) near the swim bladder.[12,17] This posture control through body flexion relies on the presence of the swim bladder, a gas-filled chamber in the body: postural recovery is impaired in swim bladder-deflated larvae.[12] Biomechanics

underlying this postural recovery has been proposed.[12] The body flexion during roll tilt displaces the swim bladder to one side while placing the head and tail to the other side. Since the density of the swim bladder is orders of magnitude lower than the rest of the body, this asymmetric positioning of the swim bladder results in the misalignment of gravity and buoyancy forces, which generates a corrective moment of force for postural recovery. This fine and static posture control strategy may be utilized by many fish species possessing a swim bladder or low-density tissue. However, adult fish differ from larvae in musculoskeletal structure, body size, and behavioral dynamics,[18–24] raising questions about the generality of this mechanism.

In the present study, behavioral analyses reveal that adult zebrafish utilize body flexion to correct roll-tilted posture similarly to larvae. When sustained roll tilt stimulus is applied, the body flexion persists throughout the stimulus. Crucially, swim bladder deflation disturbs postural recovery, suggesting swim bladder's critical role in maintaining static posture. These results suggest that zebrafish maintain an upright posture via the fine and static roll posture control mechanism through body flexion throughout their life.

Results

Adult zebrafish utilize body flexion to correct roll-tilted posture

To investigate how adult zebrafish maintain an upright posture, we developed a fish rotation apparatus (Figure 1A). A fish was placed in a cylindrical chamber in a dark room and subjected to postural disturbance in the roll axis. Viscous water containing methylcellulose was used to efficiently deliver roll stimulus to the fish and to slow down its behavior for easier observation. Fish's posture was simultaneously recorded by two cameras positioned at the front and dorsal sides of the chamber. Pigment-less *casper*[25]

97 fish were used as a standard fish for easier deflation of the swim bladder in later
98 experiments (see below).
99 Rotation of the chamber induced roll tilt in the fish. As previously reported in
100 larvae,[12,13,15] adult fish occasionally performed dynamic postural control behaviors
101 accompanied by swim-like vigorous body movement and fin beating. Since the present
102 study focused on static postural control behaviors, we collected trials in which fish
103 recovered posture without these dynamic movements. When a roll-tilt stimulus was
104 applied towards fish's left-down side, fish was slightly tilted to the left-down direction.
105 Simultaneously, the fish flexed its body to the right (ear-up) side (Figure 1B middle
106 column, Video S1). As the tilt stimulus progressed, head roll angle and body flexion angle
107 increased (Figure 1C). After the roll tilt stimulus reached its final angle, fish gradually
108 recovered the upright posture, while the flexed body relaxed to its original state (Figure
109 1B right column, Figure 1C, Video S1). Similar results were obtained in wild-type fish
110 (Figure S1). These results suggest that upon postural disturbance in the roll axis, adult
111 zebrafish recover an upright posture by the body flexion to the ear-up side.
112
113 Body flexion continues throughout sustained head roll tilt
114 To further clarify the relationship between the head roll tilt and body flexion, fish's
115 anterior body was rigidly restrained to a rectangular chamber using an acrylic holder in
116 fish tank water without methylcellulose, and a roll tilt stimulus was applied (Figure 2A).
117 With this setup, fish's head roll angle was directly coupled with the chamber's tilt angle
118 throughout the experiment. When a roll tilt stimulus was applied towards the fish's left-
119 down or right-down side and the tilt was kept for 3 s, fish continued the body flexion to
120 the ear-up side throughout the sustained stimulation (Figure 2B and 2C). In some trials,

121 fish exhibited swim-like lateral body undulation and tail flick to either left or right side
122 during the sustained tilt (Figure S2). As the sustained tilt stimulation was released, the
123 flexed body relaxed. These results further demonstrate the tight correlation between the
124 head roll tilt and body flexion.
125
126 Biomechanical model of postural recovery through body flexion
127 Mechanistically, how does the body flexion contribute to the roll postural recovery? A
128 biomechanical model of the posture control has been proposed in a larval fish study.[12]
129 The body flexion during roll tilt causes asymmetric positioning of the low-density swim
130 bladder relative to the whole body, resulting in the misalignment of gravity and buoyancy
131 forces, which generates a corrective moment of force for postural recovery.[12] Building
132 upon this biomechanical framework established in larval zebrafish, we developed a
133 corresponding model for adult zebrafish. In adult zebrafish, the center of mass (COM)
134 and center of volume (COV) are located near the constriction region between the anterior
135 and posterior swim bladder chambers.[11] Both COM and COV are located on the midline
136 when a fish is at rest: gravity acting on COM and buoyancy acting on COV are balanced
137 (Figure 3 left column). When tilted in the roll axis, the fish flexes its body towards the
138 ear-up side (Figure 3 middle column). The swim bladder shifts toward the ear-down side
139 relative to the whole body, while the head and tail reposition toward the ear-up side.
140 Because the swim bladder contains gas with a density orders of magnitude lower than the
141 rest of the body tissues, the ear-down side positioning of the swim bladder shifts relative
142 positions of COM and COV, which misaligns the gravity and buoyancy forces. This
143 misalignment generates a moment of force that counteracts the roll tilt, thereby restoring
144 an upright posture. According to this model, postural recovery is expected to be disturbed

145 in a swim bladder-deflated fish. Specifically, in the swim bladder-deflated fish, the
146 density of the body is nearly homogeneous. As a result, positions of the COM and COV
147 hardly separate, even when the fish performs body flexion during roll tilt (Figure 3 right
148 column). Consequently, little moment of force is generated, resulting in significantly
149 impaired postural recovery. Additionally, the swim bladder-deflated fish is expected to
150 be prone to roll tilt, since it is not able to efficiently counteract roll tilt through body
151 flexion.
152
153 Swim bladder plays a pivotal role in roll posture recovery
154 To test whether the model holds true in adult fish, as previously demonstrated in larvae,
155 we deflated swim bladder in *casper* fish and performed behavioral analysis (Figure S3).
156 To fairly evaluate the impact of swim bladder deflation, control experiments (sham
157 deflation) were also conducted: this sham procedure involved all the steps performed on
158 the deflated fish with the exception of piercing the swim bladder sac and applying
159 negative pressure to remove the bladder gases. After the sham procedure, fish initiated
160 locomotion within a few minutes, and locomotion speed recovered to levels comparable
161 to pre-procedure levels within the 10-minute recovery period (Figure S4). Furthermore,
162 when roll tilted, sham fish exhibited posture recovery behavior with kinetic parameters
163 similar to those of intact fish (see texts below, Table S1, and STAR Methods for kinetic
164 parameters). These data indicate that the sham procedure including anesthesia did not
165 significantly affect fish behaviors.
166 In response to roll tilt stimulus, sham fish flexed their body and recovered an upright
167 posture. Figure 4A (top photographs) and Video S2 show examples. When a roll-tilt
168 stimulus was applied towards the fish's right-down side, a sham fish was slightly tilted to

169 the right-down direction. Simultaneously, the fish flexed its body to the left (ear-up) side.
170 After the stimulus reached its final angle, the head roll angle decreased and the body
171 flexion relaxed to the original state (Figure 4A, right column in the top photographs).
172 In swim bladder-deflated fish experiments, when a roll-tilt stimulus was applied towards
173 the fish's left-down side, a fish was slightly tilted to the left-down direction (Figure 4B,
174 top photographs and Video S2). Simultaneously, the fish flexed its body to the right (ear-
175 up) side. In contrast to sham fish, the body flexion did not relax to the original state and
176 the head roll angle only slightly and gradually decreased, after the stimulus reached its
177 final angle (Figure 4B, right column in the top photographs).
178 To evaluate the effects of swim bladder deflation on behavioral kinetics, angles and
179 angular velocities of the head roll and body flexion were compared (Figure 4A and 4B,
180 bottom traces). In both sham and deflated fish, head roll angle increased as the roll tilt
181 stimulus angle increased. The head roll onset time was not significantly different (0.065
182 ± 0.052 s in sham; 0.176 ± 0.170 s in deflated, $p = 0.145$, Mann-Whitney U test). Based
183 on our biomechanical model described above, deflated fish were predicted to be more
184 prone to roll tilt, since they cannot efficiently counteract roll tilt through the body flexion.
185 Consistent with this model prediction, deflated fish exhibited larger maximum head roll
186 angles (Figure 4C, $p = 0.026$, Mann-Whitney U test), and showed delayed head roll peak
187 timing (2.024 ± 0.071 s in sham; 2.576 ± 0.152 s in deflated, $p = 0.002$, Mann-Whitney
188 U test) compared to sham controls.
189 More importantly, swim bladder deflation significantly impaired postural recovery
190 dynamics. While head roll angles gradually decreased in both sham and deflated fish
191 during recovery phase after reaching peak roll angles, the recovery kinetics were slower
192 in deflated fish. This difference was evident in their head angular velocity profiles: during

193 the recovery phase, sham fish showed pronounced troughs in their velocity traces
194 (asterisk in Figure 4A; note that negative velocity reflects rapid recovery movement),
195 whereas such troughs were much less evident in the traces of swim bladder-deflated fish
196 (Figure 4B). Quantitatively, the minimum head roll angular velocity was significantly
197 less negative (indicating slower recovery) in deflated fish compared to sham fish (Figure
198 4D, $p = 0.015$, Mann-Whitney U test). These data demonstrated that swim bladder plays
199 a critical role in effective postural recovery.
200 As head roll stimulus angle increased, body flexion angle also increased in both sham and
201 deflated fish. Similarly to the head roll angle changes, the onset time of body flexion was
202 not significantly different (0.238 ± 0.058 s in sham; 0.454 ± 0.208 s in deflated, $p = 0.093$,
203 Mann-Whitney U test), while the peak time was delayed in deflated fish (2.087 ± 0.124 s
204 in sham; 3.304 ± 0.628 s in deflated, $p = 0.004$, Mann-Whitney U test). There was no
205 significant difference in the maximum body flexion angle (Figure 4E, $p = 0.937$, Mann-
206 Whitney U test).
207 In sham fish, as the stimulus approached the final angle, the body flexion angle began to
208 decrease toward the baseline. In deflated fish, in contrast, the body flexion angle remained
209 high and did not immediately return to the baseline. As described above, sham fish
210 exhibited faster head roll recovery compared to deflated fish. Consequently, the speed of
211 body flexion relaxation was also faster: sham fish exhibited pronounced troughs in their
212 angular velocity traces (double asterisks in Figure 4A; note that negative velocity reflects
213 rapid body relaxation), whereas such troughs were barely detectable in the traces of swim
214 bladder-deflated fish (Figure 4B). The minimum body flexion angular velocity was
215 significantly less negative (indicating slower body relaxation) in the deflated fish group
216 (Figure 4F, $p = 0.002$, Mann-Whitney U test). These results demonstrated that deflating

217 the swim bladder disturbs posture recovery despite fish performing sustained body
218 flexion during roll tilt. Collectively, these findings suggest that adult zebrafish, similar to
219 larvae, employ body flexion for static roll posture control, where the swim bladder plays
220 a crucial role in effective posture recovery.
221
222 Body flexion with intact swim bladder generates recovery moment of force
223 To examine whether body flexion with intact swim bladders generates moment of force,
224 we analyzed passive movement of chemically fixed, body-flexed fish specimens before
225 and after swim bladder deflation. Fish were euthanized and chemically fixed in a body-
226 flexed posture (Figure 5A, top). The body flexion angles (θ1 in Figure 5A) were between
227 14 and 24 degrees in the 4 specimens examined. The fixed fish specimen was held by a
228 pair of forceps in a chamber filled with fish tank water. To mimic the body orientation of
229 live fish during roll tilt (Figure 1 and 4), the fixed specimen was held in a roll-tilted
230 orientation with its body flexed to the ear-up side (Figure 5A, bottom). Care was taken to
231 apply equivalent roll tilt angles (θ2 in Figure 5A) across before-deflation and after-
232 deflation conditions (before deflation: 24.3 ± 4.7°; after deflation: 24.0 ± 5.5°). The tilted
233 specimen was gently released and passive movement was recorded by a front camera.
234 Once the constraint by the forceps was removed, the specimen before swim bladder
235 deflation started passive rolling toward the ear-up side (Figure 5B, top photographs and
236 Video S3). This movement was consistent with the biomechanical model (Figure 3) and
237 was similar to postural recovery of intact and sham fish (Figures 1 and 4A). A key
238 difference between intact/sham fish and chemically fixed specimens was the presence or
239 absence of body straightening during postural recovery. In intact and sham fish, the body
240 returns to the symmetric, straight shape as the head roll angle approaches zero (Figure 1B

241 and 1C), which erases recovery moment of force and allows fish to settle into an upright
242 roll posture. In chemically fixed specimens with body-flexed shape, the body flexion
243 angle remains constant regardless of head roll angle, which likely generates moment of
244 force that keeps the specimen rolling passing through upright orientation. As expected,
245 the fixed specimens continued rolling even after they reached an upright orientation, and
246 head roll angle continuously decreased (asterisk in Figure 5C, left panel). Similar
247 movements were observed in all 4 fish specimens (asterisk in Figure 5C, right panel).
248 To examine whether swim bladder deflation disturbs the passive roll recovery, after the
249 passive movement experiments described above, the swim bladder was deflated and the
250 specimens were again subjected to the same passive movement experiments. Deflated
251 specimens did not consistently roll toward the ear-up direction (Figure 5B, bottom
252 photographs and Video S3): they did not roll or slightly rolled in a random direction
253 (double asterisks in Figure 5C, left panel). Similar movements were observed in all 4 fish
254 specimens (double asterisks in Figure 5C, right panel). Head roll angular velocities were
255 calculated from the period from 0.2 to 0.5 s after the release. Angular velocity was
256 significantly reduced after swim bladder deflation (before deflation: -290.0 ± 48.4°/s;
257 after deflation: 31.0 ± 111.2°/s; p = 1.3e-22, Welch's t-test). These results further
258 demonstrated that body flexion with intact swim bladders is sufficient to produce passive
259 recovery moment of force for roll postural recovery.
260
261 Discussion
262 The present study has established an experimental paradigm for analyzing roll postural
263 control behavior in adult zebrafish and demonstrated that when slightly roll tilted, adult
264 zebrafish exhibit body flexion to recover an upright posture (Figure 1). Both the tight

correlation between body flexion and head roll angle (Figure 2) and the dependence on swim bladder for postural recovery (Figure 4) suggest that the mechanisms underlying roll postural maintenance through body flexion are similar to those in larvae (Figure 3).[12] The passive movement experiment using chemically fixed fish specimens demonstrated that the flexed body with intact swim bladder generates recovery moment of force (Figure 5). The conservation of these mechanisms between larvae and adults suggests that body flexion serves as a fundamental strategy for static roll postural maintenance throughout their life.

Previous researches on larvae suggested that the otolith organs in the vestibular system sense roll tilt and induce the body flexion. [12,13,15,16] Not only the otolith system, but fish may also use sensory information from eyes, semicircular canals, and lateral line, to perform the body flexion during roll tilt. In our experiments, however, the body flexion was observed in dark conditions. Therefore, visual inputs are not necessary for the body flexion. Moreover, in restrained behavioral experiments, fish maintained the body flexion throughout the sustained tilt stimulus, during which angular velocity and water flow were minimal, while gravitational input from otolith organs persisted. This observation suggests that the gravity-sensing otolith organs play a primary role in inducing this behavior.

Neural circuits and muscles that induces the body flexion behavior during roll tilt were identified in zebrafish larvae.[12,13,16,17,26,27] A vestibular nucleus (tangential nucleus) receives head roll tilt signals from vestibular primary afferents and send neural signals to a group of reticulospinal neurons in the nucleus of the medial longitudinal fasciculus that projects to the spinal cord.[12] These neuronal nuclei also exist in adult fish.[28–30] This conservation of the neuronal nuclei and similarity of the body flexion behavior between

289 larvae and adults suggest that the same neural circuits likely play a principal role in
290 inducing the body flexion in adult fish. Regarding the muscles responsible for the body
291 flexion during roll tilt, adult zebrafish appeared to flex their body near the middle of the
292 body where the caudal chamber of the swim bladder is located (Figure 1B and 2B). In
293 larvae, muscle contraction during roll tilt also appears to occur only near the swim
294 bladder.[12] Consistent with this, the PHM muscles lateral to the swim bladder generate
295 body flexion, with slow-type PHM primarily responsible for this movement.[12,17] These
296 data suggest that the slow-type PHMs also generate the body flexion in adults. Muscular
297 organization in adult fish, however, is more complex and extensively developed
298 compared to larvae.[18,20,31,32] Thus, other muscles, such as trunk slow muscles that are
299 recruited during weak and sustained body movements, may also contribute to the body
300 flexion.[33] Experimentally examining the causal relationship between the body flexion and
301 neuromuscular cell populations in adult fish is technically challenging due to their size,
302 opaque tissues, ossified skull, and lack of gene promoters for selectively targeting a
303 specific cell population. However, future advancements in technology, including optical,
304 genetic, and chemical approaches, as well as combination of these, may help overcome
305 these limitations and clarify neural and muscular mechanisms.
306 In a biomechanical model, the body flexion toward the ear-up side displaces the low-
307 density swim bladder toward the ear-down side, resulting in separation of the COM and
308 COV (Figure 3). The magnitude of the recovery moment of force is proportional to the
309 distance between the COM and COV, which is maximized under a condition where the
310 swim bladder, the least dense part of the body, is located near the COM, and the body
311 flexes at the position near the swim bladder. The body organization and the body flexion
312 in larval zebrafish meet this condition, indicating that the body flexion is a reasonable,

313 energy-efficient behavior for postural correction.[12] Similarly in adult zebrafish, the
314 COM—positioned at approximately one third of the total body from the rostral end—is
315 located around a constriction region of the swim bladder separating the rostral and caudal
316 chambers.[11] Regarding the body flexion region, as discussed above, the body flexed
317 around the middle of the body (Figures 1B, 2B, 4A and 4B), the location of which was
318 slightly caudal to the swim bladder. Thus, the flexion region seems to slightly caudally
319 deviate from the most biomechanically efficient location. This subtle deviation may be
320 attributed to the musculoskeletal organization in adult fish. In the abdominal region in the
321 rostral body, bony structures increase the body stiffness: lateral angular stiffness of the
322 vertebral column is higher in the abdominal region than the caudal body region,[34] and the
323 rib cage bones covering internal organs presumably increase the stability in the abdominal
324 region. These morphological characteristics make the rostral body flexion challenging
325 and constrain the flexion region primarily to the middle and caudal body.[35,36] Considering
326 these morphological constraints, the flexion at the middle of the body is presumably an
327 adaptive compromise between biomechanical efficiency and structural limitations. While
328 the results from the swim bladder deflation experiments in live fish (Figure 4) and fixed
329 fish specimens (Figure 5) supported the biomechanical model (Figure 3), the precise
330 locations of the COM and COV during body flexion have not been provided. Further
331 investigation through morphometric analyses would help address these questions.
332 Swim bladder-deflated fish were prone to roll tilt, and their maximum head roll angle was
333 larger than sham control (Figure 4C). Previous studies showed that larval zebrafish
334 increase body flexion angle in response to increasing vestibular stimulus mimicking head
335 roll.[15,16] Given that larval and adult zebrafish employ similar roll posture control
336 mechanisms, deflated adult zebrafish in the present study would attempt to counteract roll

337 tilt by increasing their body flexion angle. However, the maximum body flexion angle
338 was comparable between control and deflated groups, despite deflated fish experiencing
339 greater postural perturbations (Figure 4E). These data suggest that adult fish face
340 morphological constraints that limit their compensatory body flexion capacity. Unlike
341 flexible larvae, adult fish possess increased body stiffness due to ossified skeletal
342 structures. This may restrict the range of achievable body flexion angles in adult fish.
343 Previous studies showed that during tilt in the roll axis, fish exhibit body undulation with
344 asymmetric motor pattern that recovers their posture.[4,5,8] Consistently, in the present
345 study, swim-like vigorous body movement and fin beating were observed when adult
346 zebrafish was roll tilted. Intriguingly, in experiments where the fish's rostral body was
347 restrained and sustained tilt stimulation was delivered, fish occasionally exhibited a
348 swim-like body undulation and tail flick behaviors in addition to their body flexion as
349 larvae do (Figure S2).[13,15,16] This indicates that fish maintain roll posture primarily
350 through static control via body flexion, and recruit dynamic control through vigorous
351 body movements when static control alone is insufficient.
352 What are the advantages of static posture control through body flexion? Compared to
353 swimming and fin movements, maintaining posture through slight body flexion is less
354 visually conspicuous and therefore likely reduces the risk of being detected by
355 predators.[37,38] Additionally, body flexion presumably requires less energy compared to
356 vigorous axial undulation during swimming.[39] This is particularly beneficial during rest
357 periods when maintaining postural stability while conserving energy is crucial.
358 The mechanism of posture control by body flexion is likely a widely used strategy
359 employed by many aquatic organisms with low-density organs. While our study focused
360 on the swim bladder, not only the swim bladder in many fish species, but also lungs in

lungfish and lipid-rich liver in sharks may play a crucial role when these animals flex their body upon roll tilt.[40–42] Further investigation across a broader range of species will elucidate the generality of the body flexion-mediated, static roll posture control mechanism.

Limitations of the study

Swim bladder-deflated fish showed slow but noticeable posture recovery (Figure 4). Technical limitations in the deflation procedure might explain this slow recovery: the swim bladder may not have been fully deflated. While the posterior chamber of the swim bladder was deflated, the anterior chamber was difficult to observe and therefore its deflation was not confirmed. Small amount of residual gas might have generated a small recovery moment of force during body flexion. In the fixed specimen experiments, since specimen viability was not a concern, we were able to apply stronger negative pressure to more extensively remove gas from the swim bladder. This might have produced more pronounced impairment of posture recovery (Figure 5).

Most behavioral experiments were conducted in viscous water conditions using methylcellulose in order to efficiently deliver roll tilt stimulus and clearly observe posture control responses. Due to the increased viscosity, the behavioral kinematic profiles measured under viscous water conditions were likely slowed relative to those under normal water conditions. The viscous medium may also affect the relative contributions of static versus dynamic postural control strategies, as the increased drag forces could favor sustained postural adjustments over rapid swimming movements. However, fish exhibited body flexion during roll tilt under normal water condition in our restrained experiments (Figure 2), and experiments using chemically fixed specimens demonstrated

that the fundamental body flexion mechanism operates effectively in normal water, suggesting that while the temporal dynamics and the relative contributions of static versus dynamic postural control strategies may be altered by viscosity, the underlying biomechanical principles remain valid.

Although the present study has demonstrated that body flexion plays a crucial role in roll posture control, this mechanism represents only one component of the complex postural control repertoire that fish employ to maintain an upright posture. Previous studies on fish postural control have primarily focused on dynamic control mechanisms. Fin movements vary considerably among fish species. Some species skillfully control their fins to maintain posture even while they do not locomote.[43–45] In these species, fin movements, particularly the pectoral fins, may play a primary role in maintaining posture. The present study focused on static posture control and did not provide quantitative analysis of the relative contributions and frequencies of static versus dynamic control strategies. As discussed above, some fish species may predominantly use dynamic posture control. Given that fish species have evolved diverse survival strategies across various aquatic environments, future comparative studies examining how postural control strategies vary among species with different body morphologies and ecological niches would provide important insights into the adaptive significance of static versus dynamic postural control mechanisms.

Resource availability

Lead contact

Further information and requests for resources and reagents should be directed to and will be fulfilled by the Lead Contact, Masashi Tanimoto (tanimoto@nibb.ac.jp).

Materials availability

This study did not generate new unique reagents.

Data and code availability

All data reported in this paper will be shared by the lead contact upon request. All original code has been deposited at Zenodo at https://zenodo.org/records/14551001 and is publicly available as of the date of publication. Any additional information is available from the lead contact upon request.

Acknowledgements

The authors are grateful to Higashijima lab members for their help with fish care and discussion. This work is supported by Japan Society for the Promotion of Science KAKENHI Grant Numbers JP20K06866 and JP23K05983.

Author contributions

R.N., T.K., S.H., and M.T. designed the research; T.K. built a prototype of the experimental apparatus under the supervision of M.T.; R.N. established the apparatus, performed experiments, and analyzed data under the supervision of M.T.; R.N. and M.T. wrote the manuscript.

Declaration of interests

The authors declare no competing interests.

433 STAR Methods

434 Key resources table

435

436 EXPERIMENTAL MODEL AND STUDY PARTICIPANT DETAILS

437 *Fish*

438 Adult wild-type and *casper*[25] zebrafish (38-45 mm in total length) were maintained under
439 light-dark cycles (10:14 or 12:12 hours) under standard conditions.[46] For all experiments,
440 both sexes of fish that displayed normal body morphology and maintained a dorsal-up
441 posture while at rest were used. For unrestrained behavioral experiments of intact fish, 2
442 males and 2 females of *casper* fish and 2 males and 2 females of wild-type fish were used.
443 For restrained behavioral experiments, 2 males and 1 female of wild-type fish and 1 male
444 and 2 females of *casper* fish were used. For unrestrained behavioral experiments of
445 *casper* fish with swim bladder deflation, 3 males and 3 females were used for sham
446 deflation, and 3 males and 3 females were used for deflation. For locomotion experiments,
447 1 male and 3 females of *casper* fish were used. For fixed specimen passive movement
448 experiments, 2 males and 2 females of *casper* fish were used. All experiments were
449 conducted according to animal experiment protocols approved by the animal care and use
450 committees of the National Institutes of Natural Sciences.

451

452 METHODS DETAILS

453 *Unrestrained behavioral experiments*

454 The fish chamber consisted of two acrylic cylinders of different sizes (22 mm [inner
455 diameter] × 50 mm [length] × 1.5 mm [thickness] and 46 mm [inner diameter] × 10 mm
456 [length] × 2 mm [thickness]) connected by an acrylic ring plate. The two cylinders were

457 separated by a transparent, fluorinated ethylene propylene sheet (NR0538-002,
458 Fronchemical), which had similar refractive index as water. Small holes were made on
459 this sheet so that water passes between the two cylinders. Both ends of the connected
460 chamber were covered with acrylic lids. The two cylinders served different purposes: the
461 smaller cylinder housed a fish, while the larger cylinder supplied oxygen and, by
462 manually tilting the chamber, removed small air bubbles from the smaller cylinder. Air
463 bubble was maintained in the larger cylinder for oxygen supply. Since it was difficult to
464 consistently tilt adult fish and reliably observe their postural responses in normal water
465 conditions, presumably due to their large inertia and rapid postural recovery, behavioral
466 experiments were conducted under viscous water conditions. The chamber was filled with
467 fish tank water containing 0.8% methylcellulose (22223-65, Nacalai Tesque, inc.), and a
468 fish was placed in the smaller cylinder.
469 The rotation stimulus device was composed of a motorized rotation stage (DDR100/M,
470 ThorLabs) and supporting mechanical components. The fish chamber was mounted on
471 this device. The stage was driven by a stage controller (BBD301, ThorLabs) using a
472 software (Kinesis version 1.14.49, ThorLabs). Fish were illuminated by an infrared light-
473 emitting diode (IR-LED) plate (LFL-100IR2-850, CCS) from the ventral side and another
474 IR-LED (HLV3-22IR860, CCS) from the caudal side. Experiments were conducted in a
475 dark room to eliminate visual cues. The chamber was rotated 45° in the roll direction
476 (maximum velocity: 40°/s, acceleration and deceleration: 25°/s^2) unless otherwise noted.
477 Fish behavior was recorded at 60 frames per s (fps) by two cameras (HC-VX992MS,
478 Panasonic) from the frontal and dorsal sides. The timing of rotation stimulus and camera
479 image frames were synchronized by a flash of an IR-LED, which was oriented towards
480 two cameras and distinct from the illumination IR-LEDs. In each trial, a voltage pulse

481 was sent from the rotation stage controller to the IR-LED through a pulse generator
482 (SEN7203, Nihon Kohden) at 1 s before the rotation started.
483 Since swim bladder-deflated fish were prone to roll tilting, they exhibited dynamic
484 posture control through swimming and tail flick more frequently compared to intact and
485 sham fish when subjected to the standard roll stimulation described above. To better
486 observe static posture control via slight body flexion, a weaker rotation stimulus of 35-
487 45° (maximum velocity: 30-40°/s, acceleration and deceleration: 20-25°/s²) was applied.
488 The reduced buoyancy caused by swim bladder deflation was compensated by 5-32% (in
489 most cases 10-25%) sucrose (196-00015, Fujifilm Wako), depending on neutral buoyancy
490 of individual fish, in fish tank water containing 0.8% methylcellulose (22223-65, Nacalai
491 Tesque, inc.) solution. For wild-type fish, which were slightly larger than *casper* fish, a
492 cylinder chamber with larger dimensions (26 mm [inner diameter] × 50 mm [length] × 2
493 mm [thickness] and 46 mm [inner diameter] × 10 mm [length] × 2 mm [thickness]) was
494 used.
495
496 *Swim bladder deflation*
497 Pigment-less *casper* fish were used for easier identification of the swim bladder position.
498 Fish were anesthetized with 0.01% MS-222 (Ethyl 3-aminobenzoate methanesulfonate,
499 A5040, Sigma-Aldrich) for 10 minutes, and after confirming the absence of response to
500 tactile stimuli, a syringe needle (27G [NN-2719S, Terumo] or 30G [Dentronics]) was
501 gently inserted into the caudal chamber of the swim bladder from a lateral and slightly
502 dorsal and caudal direction. Negative pressure was gently and gradually applied to the
503 syringe to remove the gas from the swim bladder. Successful swim bladder deflation was
504 confirmed by the caudal chamber of the swim bladder becoming invisible. Following

505 deflation, fish were returned to tank water, allowed to rest for 10 minutes before
506 behavioral experiments.
507
508 *Sham deflation*
509 Sham swim bladder deflation was performed almost exactly as those for deflation
510 procedure described above. The only modification was that the swim bladder sac was not
511 penetrated by a syringe needle and swim bladder gas was not removed for sham deflation.
512 Even slight piercing of the swim bladder sac with a syringe needle resulted in gas leakage,
513 which would have compromised the intended control condition. Therefore, sham fish
514 underwent identical handling, surgical preparation, and recovery procedure to those used
515 for deflated fish, but with the swim bladder left intact avoiding penetration of the swim
516 bladder sac.
517
518 *Locomotion before and after sham deflation procedure*
519 *casper* fish were used. Individual fish was placed in a tank (260 mm [length] × 150 mm
520 [width] × 175 mm [height]) filled with fish tank water (depth: 70 mm), and behavior was
521 recorded at 60 fps for 11 minutes from the top by a camera (HC-VX992MS, Panasonic).
522 Sham swim bladder deflation was performed as described above. After the sham
523 procedure, fish was again placed in the tank and behavior was recorded.
524
525 *Restrained behavioral experiments*
526 Fish were anesthetized with 0.01% MS-222 for 10 minutes. The fish's body between the
527 operculum and pectoral fin was immobilized by a separable pair of acrylic plates that
528 have a ditch: an elliptical hole (major axis: 6.0-6.75 mm; minor axis: 4-5 mm) was formed

529 when these plates were combined together. To stabilize the body position, a small amount
530 of flexible silicone (Macks Earplugs) was applied to the space between the hole and the
531 fish body. The plate holding the fish was then placed into a groove of an acrylic chamber
532 (60 mm [length] × 30 mm [width] × 45 mm [height]) filled with fish tank water without
533 methylcellulose. An open-topped rectangular box (55 mm [length] × 30 mm [width] × 20
534 mm [height]) was placed over the fish to prevent image distortion when tilt stimulus was
535 applied and the water surface tilted. Fish were allowed to rest for at least a few minutes
536 before stimulus delivery and camera recording began. Fish was illuminated by an IR-LED
537 (LFL-100IR2-850, CCS) placed below the chamber. The rotation stimulus device was the
538 same as that described in 'Unrestrained behavioral experiments' section. The chamber
539 was mounted on the rotation stimulus device, and 20° roll-tilt stimulation (maximum
540 velocity: 10°/s, acceleration and deceleration: 5°/s²) was applied and held for 3 s before
541 returning to its original position. Fish behavior was recorded at 25 fps by a camera
542 (daA720-520um, Basler) with a lens (13VM308ASIRII, Tamron) from the dorsal side
543 using software (pylon Viewer version 6.2.0.8205, Basler). The camera tilted together with
544 the fish chamber. The timing of the rotation stimulus and the camera image frames were
545 synchronized by voltage pulses. Specifically, from 2 s before the rotation started in each
546 trial, image frame acquisition was triggered by voltage pulses from the rotation stage
547 controller through a pulse generator (SEN-7203, Nihon Kohden).
548
549 *Fixed-specimen passive movement experiments*
550 Fish were euthanized by placing them with 0.04% MS-222 for 30 minutes. The fish
551 specimens were restrained on a sponge plate using metal pins, with the body maintained
552 in a bent posture such that the body flexion angle was approximately 20 degrees. The

553 body bend direction was to the left in 2 fish and to the right in 2 fish. The fish specimens
554 were fixed with 4% paraformaldehyde (158127, Sigma-Aldrich) in 1x phosphate buffered
555 saline (PBS) for 30 minutes at room temperature. After brief rinse with 1x PBS, the fish
556 specimens were photographed from the dorsal direction by a camera (HC-VX992MS,
557 Panasonic). The body flexion angle of the fixed fish specimens was between 14 and 24
558 degrees in 4 specimens examined.
559 The fixed fish specimen was held by a pair of forceps in a chamber filled with fish tank
560 water. The held specimen was manually roll tilted from the dorsal-up orientation with its
561 body flexed to the ear-up side. The tilted specimen was released and passive movement
562 was recorded by a front camera (HC-VX992MS, Panasonic) at 60 fps. Care was taken to
563 minimize external forces to the specimen after the release. Swim bladder deflation was
564 performed as described above. Since specimen viability was not a concern, swim bladder
565 deflation was performed more extensively than in live fish, allowing for stronger negative
566 pressure application and more complete gas removal.
567
568 QUANTIFICATION AND STATISTICAL ANALYSIS
569 *Image analysis of live fish experiments*
570 Captured videos were analyzed with a custom program written in Python (version 3.12.7).
571 The data analysis employed Python libraries including NumPy, OpenCV, Matplotlib,
572 pandas and scikit-image[47–51]. Videos from unrestrained behavioral experiments were
573 downsampled to 30 fps, which was sufficient to capture behavioral dynamics. Videos
574 from restrained behavioral experiments were analyzed at the original frame rate. For
575 analysis, videos were converted into series of TIFF images using OpenCV. The head roll
576 angle was calculated as follows: each image from the frontal camera was binarized to

isolate pixels containing the eyes, and the xy coordinates of each eye's center were estimated. The head roll angle was then measured as the angle between the line connecting the centers of the two eyes and the horizontal line.

The body flexion angle was calculated using images from the dorsal camera. Each image was binarized to extract pixels containing the fish while excluding the fins. The fish's midline, from snout to tail, was divided into 23 segments. The body flexion angle was determined by calculating the angle between two lines: (1) the line connecting the second and twelfth points from the tail, and (2) the line connecting the twelfth and twenty-second points. These points were selected since the two lines best represent the body flexion in most cases. In image frames where the fish's snout or tail overlapped with the contour of the cylinder in the images, the point closest to the body flexion point (either the thirteenth, fourteenth, or fifteenth point) was chosen as the middle point. The angle was calculated between (1) the line connecting the second and middle points, and (2) the line connecting the middle and twenty-second points. The dorsal camera images were distorted by optical refraction through the curved surface of the acrylic cylinder, resulting in slight expansion of image objects in the cylinder's short-axis direction. The magnitude of distortion increased from the top to the bottom of the cylinder along the depth axis. It also increased from the center to the edge along the cylinder's short-axis direction in horizontal planes, except in the middle horizontal planes where the image slightly shrank near the cylinder's edge. However, since the body flexion angle was measured from the body midline, this image distortion would minimally affect the angle measurements. Also, since the fish's location was randomly distributed in the cylinder across multiple trials, any potential effects of image distortion would be averaged out, thus having minimal impact on the angle analysis. Therefore, the body flexion angle was calculated from raw images.

For all measurements except dynamic movement analysis (Figure S2), image frames where fish exhibited swimming or tail flick were excluded from the dataset. Supplementary videos were made from image series using a software (Clipchamp, Microsoft).

Image analysis of locomotion experiments

Captured videos were analyzed with a custom program written in MATLAB (version R2023a). In each image frame, background was subtracted, binarized to find pixels containing fish, and the centroid position was estimated. Instantaneous locomotion speed was calculated from the centroid position changes and smoothed by 60-frame moving average. Locomotion speed was then calculated as the mean instantaneous speed per minute.

Image analysis of fixed-specimen passive movement experiments

Head roll angle was calculated from captured videos using the same methods described above for live fish. Videos were analyzed at the original frame rate. For image frames where the custom tracking program failed to detect eye positions, these eye positions were manually annotated. Only trials where fish specimens showed no visible influence of external forces from the pair of forceps after release were included in the analysis. For each individual fish specimen, 10 trials each were randomly selected from the before-deflation and after-deflation conditions.

Definition of Measured Values and Statistical Analysis

Data was analyzed using a custom code written in Python (version 3.12.7). A single trial

where head roll angle exceeded more than 40 degrees was excluded from the analysis. To extract slow changes in head angle, a 21-frame moving average was applied to raw head angle data. Raw body flexion angle data was smooth enough, and therefore raw angle data was used. All time-series head roll and body flexion angle data were offset by subtracting the pre-stimulus baseline that was average angle during the initial 1 s of each trial. The maximum head roll angle and body flexion angle were defined as the peak values after the stimulus onset. Head roll angular velocity was calculated from the smoothened angle data in each trial using the numpy.gradient function from the Python NumPy library, and a 15-frame moving average was applied. For body flexion angular velocity, a 25-frame moving average was applied to raw angle data. Angular velocity was then calculated from the smoothened angle data in each trial using the numpy.gradient function, and a 13-frame moving average was applied. The minimum angular velocity was defined as the lowest value after the tilt stimulus onset. Onset time for head roll and body flexion angles were defined as the first time point at which the angles after the stimulus onset exceeded 2× standard deviation during 1 s pre-stimulus period. Peak time for head roll and body flexion angles were defined as the time point at which the angles after stimulus onset reached their maximum value. For fixed-specimen passive movement, head roll angular velocities were calculated as the slope of linear regression fitted to angle data in each trial during the period from 0.2 to 0.5 s after release. The effect of swim bladder deflation on posture recovery was evaluated by testing angular velocity values using the two-sided Welch's t-test. All statistical analyses were performed using the SciPy tool (version 1.13.1)[52]. Except the fixed-specimen passive movement analysis, the mean value for each individual was calculated from in the recorded trials. Using the individual means, the overall mean and standard deviation were calculated for intact,

649 sham, and swim bladder-deflated fish. The effect of swim bladder deflation on posture
650 recovery was evaluated using the two-sided Mann-Whitney U test.
651
652 Supplemental information
653 Figure S1. Unrestrained behavioral experiments in wild-type fish, related to Figure 1.
654 Figure S2. Dynamic movement during roll tilt, related to Figure 2.
655 Figure S3. Swim bladder deflation, related to Figure 4.
656 Figure S4. Locomotion before and after sham deflation procedure, related to Figure 4.
657 Table S1. Kinematic parameters in intact, sham, and deflated fish, related to Figure 4.
658 Video S1. Static posture control by body flexion during roll-tilt stimulus in intact adult
659 *casper* zebrafish, related to Figure 1
660 Video S2. Static posture control by body flexion during roll-tilt stimulus in sham deflation
661 and swim bladder-deflated adult *casper* zebrafish, related to Figure 4
662 Video S3. Passive movement of fixed fish specimens before and after swim bladder
663 deflation, related to Figure 5
664
665 Figure legends
666 Figure 1. Static roll posture control through body flexion in adult zebrafish.
667 (A) Schematic illustration of unrestrained behavioral experiments. Behavior of adult
668 zebrafish during roll tilt stimuli was recorded using dorsal and frontal view cameras in a
669 dark room. (B, C) Behavioral experiments on intact adult *casper* fish. (B) Snapshots of a
670 fish during a roll tilt stimulus towards its left-down side (top row: frontal view; bottom
671 row: dorsal view). Magenta lines connecting the center of eyes show head roll angle.
672 Black and magenta dashed lines denote the midlines of the rostral and caudal body,

respectively. Changes in the head roll angle and body flexion angle relative to the pre-stimulus baselines are indicated at the upper right. Fish tank water contains methylcellulose. Before stimulus onset, the fish maintains an upright posture (0.0 s). As the fish is tilted in the roll direction, it flexes its body towards the ear-up side (2.5 s). The fish recovers its upright posture as it straightens its body (6.0 s). Scale bars indicate 3 mm. (C) Time courses of changes in head roll angle and body flexion angle in response to roll tilt stimuli. Average traces from four individual fish are shown in different colors (7 to 9 trials per fish). See also Figures S1.

Figure 2. Restrained behavior during static roll tilt.

(A) Schematic illustration of restrained behavioral experiments. A fish was restrained and subjected to roll tilt stimuli in a dark room. Its behavior was recorded by a dorsal camera, which tilted together with the fish chamber. (B) Snapshots of a restrained fish during a roll tilt stimulus towards its left-down side. Before stimulus onset, the body is straight (-2.0 s). While the sustained tilt stimulus is applied, the fish maintains body flexion (6.0 s). As the tilt stimulus is released, the fish straightens its body (12.0 s). Scale bars indicate 3 mm. (C) Time courses of body flexion angle in response to roll tilt stimuli. Average traces from six individual fish (5 to 8 trials per fish) are shown (red: *casper* fish; blue: wild-type fish). See also Figure S2.

Figure 3. A mechanistic model of static roll posture control through body flexion in adult fish.

A biomechanical model of postural recovery from roll tilt by body flexion adapted from a model for larval zebrafish in Sugioka et al.[12] Gravity and buoyancy forces act at the center of mass (COM) and center of volume (COV), respectively. The COM and COV are located near the constriction region between the anterior and posterior swim bladder chambers.[11] Left column: At rest, the fish's COM and COV are located on the midline, and the gravity and buoyancy forces are nearly balanced, enabling the fish to maintain an upright posture. Middle column: When the fish is tilted in the roll direction, it flexes its body towards the ear-up side, causing the swim bladder to shift towards the ear-down side. The extremely low density of the swim bladder results in a shift in the relative positions of the COM and COV. This misalignment of gravity and buoyancy axes generates a moment of force that restores the upright posture. Right column: A fish with a deflated swim bladder flexes its body when tilted in the roll direction. Due to nearly uniform body density, the relative position of COM and COV remains almost unchanged. Consequently, the moment of force is greatly reduced, preventing restoration of upright posture.

Figure 4. Behavior of static roll posture control in swim bladder-deflated fish.

(A and B) Behavioral images and kinetics of sham control and swim bladder-deflated *casper* fish. (Top photographs) Snapshots of a sham fish (A) and swim bladder-deflated fish (B) during a roll tilt stimulus (top row: frontal view; bottom row: dorsal view). Fish

721 tank water contains methylcellulose (A) and methylcellulose and sucrose (B). A sham
722 fish maintains an upright posture before stimulus onset (0.0 s). As the fish is tilted in the
723 right-down direction, it flexes its body towards the left (ear-up) side (2.5 s). The fish
724 recovered upright posture, while its body flexion relaxed to the original state (6.0 s). A
725 deflated fish maintains an upright posture before stimulus onset (0.0 s). As the fish is
726 tilted in the left-down direction, it flexes its body towards the right (ear-up) side (2.5 s).
727 The fish remains roll tilted, while it continues body flexion (6.0 s). Scale bar indicates 3
728 mm. (Bottom traces) Time courses of changes in head roll angle, head roll angular
729 velocity, changes in body flexion angle, and body flexion angular velocity in response to
730 roll tilt stimuli. Average traces from six individual fish are shown in different colors (4 to
731 8 trials per fish). In angular velocity traces of head roll and body flexion, there are troughs
732 (asterisk and double asterisks) during postural recovery in sham fish group, while troughs
733 are not clearly observed in deflated fish group. (C-F) Comparison of behavioral
734 parameters between sham group and swim bladder-deflated group. (C) Maximum head
735 roll angle. $p = 0.026$, Mann-Whitney U test. (D) Minimum head roll angular velocity. p
736 $= 0.015$, Mann-Whitney U test. (E) Maximum body flexion angle. $p = 0.937$, Mann-
737 Whitney U test. (F) Minimum body flexion angular velocity. $p = 0.002$, Mann-Whitney
738 U test. See also Figures S3 and S4.
739
740
741
742 Figure 5. Fixed-specimen passive movement experiments.
743 (A) Schematic illustration of fixed-specimen passive movement experiments. A fish was
744 euthanized and chemically fixed in a body-flexed posture with body flexion angle (θ1)

745 approximately 20 degrees. The fixed fish specimen was held by a pair of forceps in a
746 chamber filled with fish tank water. The held specimen was manually roll tilted
747 approximately 24 degrees (θ2) with its body flexed to the ear-up side. The tilted specimen
748 was released and passive movement was recorded by a front camera. (B) Snapshots of
749 passive movement of a released fish specimen before (top row) and after (bottom row)
750 swim bladder deflation. Before deflation, the specimen rolls toward ear-up side and
751 continues rolling. After deflation, the specimen does not roll. Scale bar indicates 3 mm.
752 (C) Time courses of head roll angle before (asterisk) and after swim bladder deflation
753 (double asterisks). (Left) Ten trials in each condition from an example fish. (Right) Data
754 from 4 fish. Black traces represent mean and gray areas represent standard deviation.
755
756
757 Figure S1. Unrestrained behavioral experiments in wild-type fish.
758 (A, B) Unrestrained behavioral experiments in wild-type adult zebrafish performed in a
759 dark room. (A) Snapshots of a fish during a roll tilt stimulus towards its left-down side
760 (top row: frontal view; bottom row: dorsal view). Magenta lines connecting the center of
761 eyes show head roll angle. Black and magenta dashed lines denote the midlines of the
762 rostral and caudal body, respectively. Changes in the head roll angle and body flexion
763 angle relative to the pre-stimulus baselines are indicated at the upper right. Before
764 stimulus onset, the fish maintains an upright posture (0.0 s). As the fish is tilted in the roll
765 direction, it flexes its body towards the ear-up side (2.5 s). The fish recovers its upright
766 posture as it straightens its body (5.0 s). Scale bars indicate 3 mm. (B) Time courses of
767 changes in head roll angle and body flexion angle in response to roll tilt stimuli. Average
768 traces from four individual fish are shown in different colors (6 to 9 trials per fish).

Figure S2. Dynamic movement during roll tilt.

Time course of body flexion angle in response to sustained roll tilt stimulation in body-restrained experiments. Example 5 trials where fish exhibited dynamic movement are shown in different colors.

Figure S3. Swim bladder deflation.

Lateral view images of pigment-less *casper* fish before and after swim bladder deflation. Scale bar indicates 5 mm.

Figure S4. Locomotion before and after sham deflation procedure.

Average locomotion speed per minute before and after sham deflation procedure. Locomotion speed recovered to levels comparable to pre-procedure levels in a few minutes.

Table S1. Kinematic profiles of head roll and body flexion in intact, sham, and deflated fish.

Kinematic parameters in intact, sham, and deflated fish (mean ± standard deviation). N indicates number of fish. Mann-Whitney U test was used for statistic comparisons. U denotes the test statistic. Asterisks indicate p values smaller than 0.05.

Video S1. Static posture control by body flexion during roll-tilt stimulus in intact adult zebrafish.

Front and dorsal view video clips in intact *casper* fish. Video plays at real-time speed.

Video S2. Static posture control by body flexion during roll-tilt stimulus in sham deflation and swim bladder-deflated adult zebrafish.

Front and dorsal view video clips in sham deflation (first half) and swim bladder-deflated (second half) *casper* fish. Video plays at real-time speed.

Video S3. Passive movement of fixed fish specimens.

Front view video clips of a fixed fish specimen before (first half) and after (second half) swim bladder deflation. Video plays at ×0.25 speed.

References

1. Horak, F. B. Postural orientation and equilibrium: what do we need to know about neural control of balance to prevent falls? *Age Ageing* 35, ii7–ii11 (2006).

2. Le Mouel, C. & Brette, R. Mobility as the Purpose of Postural Control. *Front Comput Neurosci* 11, (2017).

3. Maki, B. E., Mcilroy, W. E. & Fernie, G. R. Change-in-support reactions for balance recovery. *IEEE Engineering in Medicine and Biology Magazine* 22, 20–26 (2003).

4. Zelenin, P. V., Orlovsky, G. N. & Deliagina, T. G. Sensory-Motor Transformation by Individual Command Neurons. *The Journal of Neuroscience* 27, 1024–1032 (2007).

5. Bagnall, M. W. & McLean, D. L. Modular Organization of Axial Microcircuits in Zebrafish. *Science (1979)* 343, 197–200 (2014).

6. Webb, P. W. & Weihs, D. Hydrostatic stability of fish with swim bladders: not all fish are unstable. *Can J Zool* 72, 1149–1154 (1994).

7. Ehrlich, D. E. & Schoppik, D. Control of Movement Initiation Underlies the

Development of Balance. *Current Biology* 27, 334–344 (2017).

8. Zelenin, P. V., Grillner, S., Orlovsky, G. N. & Deliagina, T. G. The pattern of motor coordination underlying the roll in the lamprey. *Journal of Experimental Biology* 206, 2557–2566 (2003).

9. Fath, M. & Tytell, E. D. Day and night posture of the bluegill sunfish (*Lepomis macrochirus*). Preprint at https://doi.org/10.1101/2023.07.13.548884 (2023).

10. Webb, P. W. & Weihs, D. Stability versus Maneuvering: Challenges for Stability during Swimming by Fishes. *Integr Comp Biol* 55, 753–764 (2015).

11. Robertson, G. N., Lindsey, B. W., Dumbarton, T. C., Croll, R. P. & Smith, F. M. The contribution of the swimbladder to buoyancy in the adult zebrafish (*Danio rerio*): A morphometric analysis. *J Morphol* 269, 666–673 (2008).

12. Sugioka, T., Tanimoto, M. & Higashijima, S. Biomechanics and neural circuits for vestibular-induced fine postural control in larval zebrafish. *Nat Commun* 14, 1217 (2023).

13. Beiza-Canelo, N. *et al.* Magnetic actuation of otoliths allows behavioral and brain-wide neuronal exploration of vestibulo-motor processing in larval zebrafish. *Current Biology* 33, 2438-2448.e6 (2023).

14. Migault, G. *et al.* Whole-Brain Calcium Imaging during Physiological Vestibular Stimulation in Larval Zebrafish. *Current Biology* 28, 3723-3735.e6 (2018).

15. Favre-Bulle, I. A., Stilgoe, A. B., Rubinsztein-Dunlop, H. & Scott, E. K. Optical trapping of otoliths drives vestibular behaviours in larval zebrafish. *Nat Commun* 8, 630 (2017).

16. Natalia Beiza Canelo. Postural control in larval zebrafish : vestibular behavior repertoire and a new method to study it. *Portail HAL Sorbonne Université* (2022).

17. Thiele, T. R., Donovan, J. C. & Baier, H. Descending Control of Swim Posture by a Midbrain Nucleus in Zebrafish. *Neuron* 83, 679–691 (2014).

18. Thorsen, D. H. & Hale, M. E. Development of zebrafish (Danio rerio) pectoral

fin musculature. *J Morphol* 266, 241–255 (2005).

19. Ma, X. & Xu, X. A Swimming-based Assay to Determine the Exercise Capacity of Adult Zebrafish Cardiomyopathy Models. *Bio Protoc* 11, (2021).

20. McMenamin, S. K. & Parichy, D. M. Metamorphosis in Teleosts. in *Current Topics in Developmental Biology* vol. 103 127–165 (Academic Press Inc., 2013).

21. McHenry, M. J. & Lauder, G. V. Ontogeny of form and function: Locomotor morphology and drag in zebrafish (Danio rerio). *J Morphol* 267, 1099–1109 (2006).

22. Burris, B., Jensen, N. & Mokalled, M. H. Assessment of Swim Endurance and Swim Behavior in Adult Zebrafish. *Journal of Visualized Experiments* (2021) doi:10.3791/63240.

23. Mauguit, Q., Olivier, D., Vandewalle, N. & Vandewalle, P. Ontogeny of swimming movements in bronze corydoras (Corydoras aeneus). *Can J Zool* 88, 378–389 (2010).

24. Gibb, A. C., Swanson, B. O., Wesp, H., Landels, C. & Liu, C. Development of the Escape Response in Teleost Fishes: Do Ontogenetic Changes Enable Improved Performance? *Physiological and Biochemical Zoology* 79, 7–19 (2006).

25. White, R. M. *et al.* Transparent Adult Zebrafish as a Tool for In Vivo Transplantation Analysis. *Cell Stem Cell* 2, 183–189 (2008).

26. Favre-Bulle, I. A., Vanwalleghem, G., Taylor, M. A., Rubinsztein-Dunlop, H. & Scott, E. K. Cellular-Resolution Imaging of Vestibular Processing across the Larval Zebrafish Brain. *Current Biology* 28, 3711-3722.e3 (2018).

27. Bianco, I. H. *et al.* The tangential nucleus controls a gravito-inertial vestibulo-ocular reflex. *Current Biology* 22, 1285–1295 (2012).

28. Straka, H. & Baker, R. Vestibular blueprint in early vertebrates. *Front Neural Circuits* 7, (2013).

29. SUWA, H., GILLAND, E. & BAKER, R. Otolith Ocular Reflex Function of the Tangential Nucleus in Teleost Fish. *Ann N Y Acad Sci* 871, 1–14 (1999).

30. K. Lee, R. K. & Eaton, R. C. Identifiable reticulospinal neurons of the adult zebrafish, *Brachydanio rerio*. *Journal of Comparative Neurology* 304, 34–52 (1991).

31. Stickland, N. C. Growth and development of muscle fibres in the rainbow trout (Salmo gairdneri). *J Anat* 137 (Pt 2), 323–33 (1983).

32. te Kronnié, G. Axial muscle development in fish. *Basic Applied Myology* 10, (2000).

33. Jayne, B. C. & Lauder, G. V. How swimming fish use slow and fast muscle fibers: implications for models of vertebrate muscle recruitment. *Journal of Comparative Physiology A* 175, (1994).

34. Nowroozi, B. N. & Brainerd, E. L. Regional variation in the mechanical properties of the vertebral column during lateral bending in Morone saxatilis. *J R Soc Interface* 9, 2667–2679 (2012).

35. TSUKAMOTO, K. Swimming motion of fishes : Their adaptation to water. *Hikaku seiri seikagaku (Comparative Physiology and Biochemistry)* 10, 249–262 (1993).

36. Hang, H., Heydari, S., Costello, J. H. & Kanso, E. Active tail flexion in concert with passive hydrodynamic forces improves swimming speed and efficiency. *J Fluid Mech* 932, (2022).

37. Martel, G. & Dill, L. M. Influence of Movement by Coho Salmon (*Oncorhynchus kisutch)* Parr on Their Detection by Common Mergansers (*Mergus merganser). Ethology* 99, 139–149 (1995).

38. Tang, Z.-H., Huang, Q., Wu, H., Kuang, L. & Fu, S.-J. The behavioral response of prey fish to predators: the role of predator size. *PeerJ* 5, e3222 (2017).

39. Gerry, S. P. & Ellerby, D. J. Resolving shifting patterns of muscle energy use in swimming fish. *PLoS One* 9, (2014).

40. McCune, A. R. & Carlson, R. L. Twenty ways to lose your bladder: common natural mutants in zebrafish and widespread convergence of swim bladder loss among teleost fishes. *Evol Dev* 6, 246–259 (2004).

41. Maina, J. N. & Maloiy, G. M. O. The morphometry of the lung of the African lungfish (*Protopterus aethiopicus*) : its structural-functional correlations. *Proc R Soc Lond B Biol Sci* 224, 399–420 (1985).

42. Baldridge, H. D. Sinking Factors and Average Densities of Florida Sharks as Functions of Liver Buoyancy. *Copeia* 1970, 744 (1970).

43. Drucker, E. G. & Lauder, G. V. Function of pectoral fins in rainbow trout: behavioral repertoire and hydrodynamic forces. *Journal of Experimental Biology* 206, 813–826 (2003).

44. Hove, J. R., O'Bryan, L. M., Gordon, M. S., Webb, P. W. & Weihs, D. Boxfishes (Teleostei: Ostraciidae) as a model system for fishes swimming with many fins: kinematics. *Journal of Experimental Biology* 204, 1459–1471 (2001).

45. Hale, M. E. Developmental Change in the Function of Movement Systems: Transition of the Pectoral Fins between Respiratory and Locomotor Roles in Zebrafish. *Integr Comp Biol* 54, 238–249 (2014).

46. Westerfield M. The zebrafish book, 5th Edition; A guide for the laboratory use of zebrafish (Danio rerio) University of Oregon Press; Eugene, Oregon: 2007.

47. Harris, C. R. *et al.* Array programming with NumPy. *Nature* vol. 585 Preprint at https://doi.org/10.1038/s41586-020-2649-2 (2020).

48. Bradski, G. (2000) The OpenCV Library. Dr. Dobb's Journal of Software Tools, 120; 122-125.

49. Hunter, J. D. Matplotlib: A 2D graphics environment. *Comput Sci Eng* 9, (2007).

50. McKinney, W. (2010) Data Structures for Statistical Computing in Python. Proceedings of the 9th Python in Science Conference, Austin, 28 June-3 July 2010, 56-61. https://doi.org/10.25080/Majora-92bf1922-00a.

51. van der Walt S, Schönberger JL, Nunez-Iglesias J et al (2014) scikit-image: image processing in python. PeerJ 2:e453. https:// doi.org/10.7717/peerj.453.

52. Virtanen, P. *et al.* SciPy 1.0: fundamental algorithms for scientific computing in Python. *Nat Methods* 17, 261–272 (2020).

Figure 1

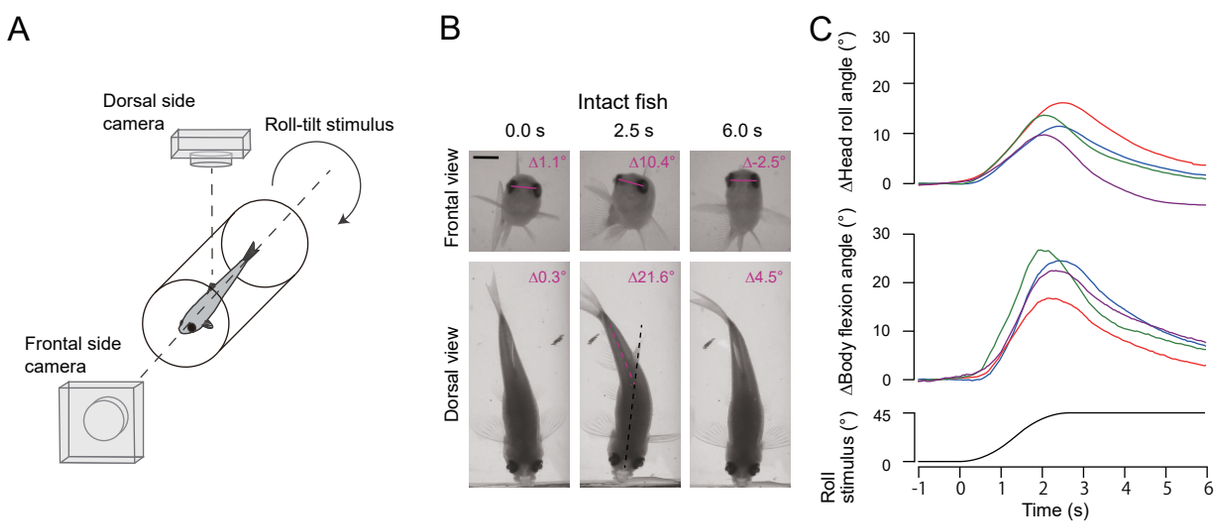
A
Dorsal side camera
Roll-tilt stimulus
Frontal side camera
B
Intact fish
0.0 s
2.5 s
6.0 s
Frontal view
Dorsal view
Δ1.1°
Δ10.4°
Δ-2.5°
Δ0.3°
Δ21.6°
Δ4.5°
C
ΔHead roll angle (°)
ΔBody flexion angle (°)
Roll stimulus (°)
Time (s)

Figure 2

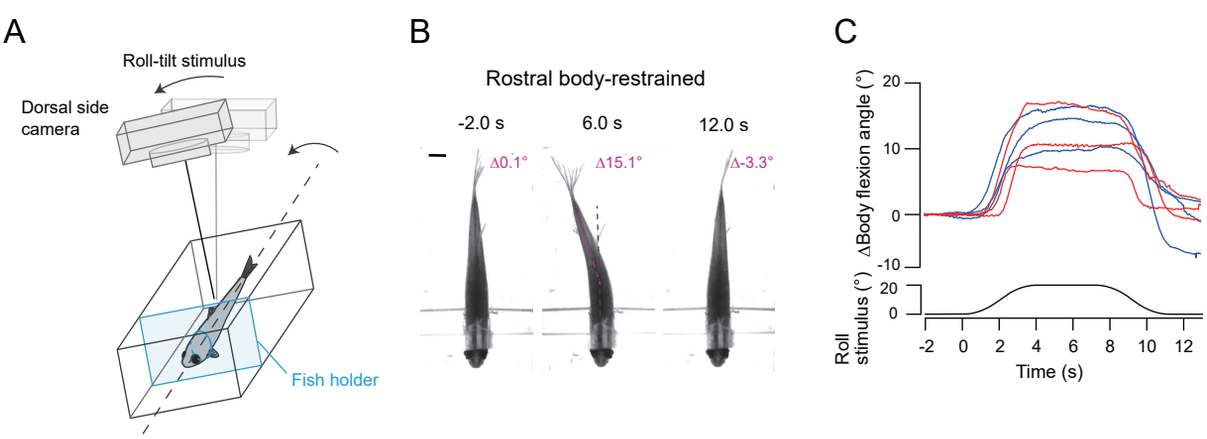
A
Roll-tilt stimulus
Dorsal side camera
Fish holder
B
Rostral body-restrained
-2.0 s
6.0 s
12.0 s
Δ0.1°
Δ15.1°
Δ-3.3°
C
ΔBody flexion angle (°)
20
10
0
-10
Roll stimulus (°)
20
0
-2
0
2
4
6
8
10
12
Time (s)

Figure 3

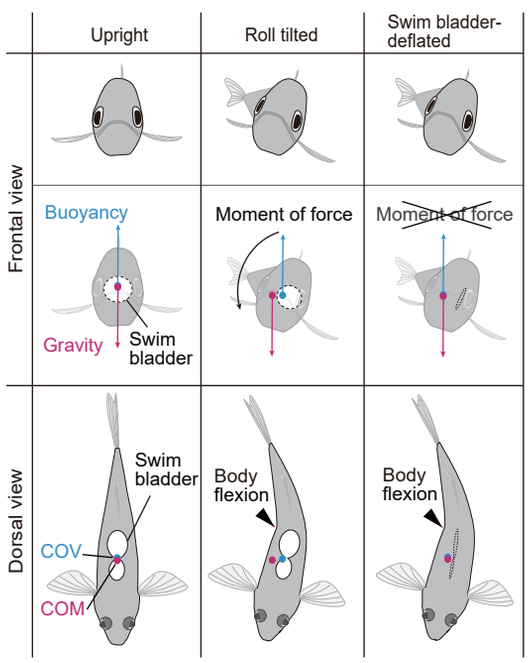
Upright
Roll tilted
Swim bladder-deflated
Frontal view
Buoyancy
Gravity
Swim bladder
Moment of force
Moment of force
Dorsal view
Swim bladder
COV
COM
Body flexion
Body flexion

Figure 4

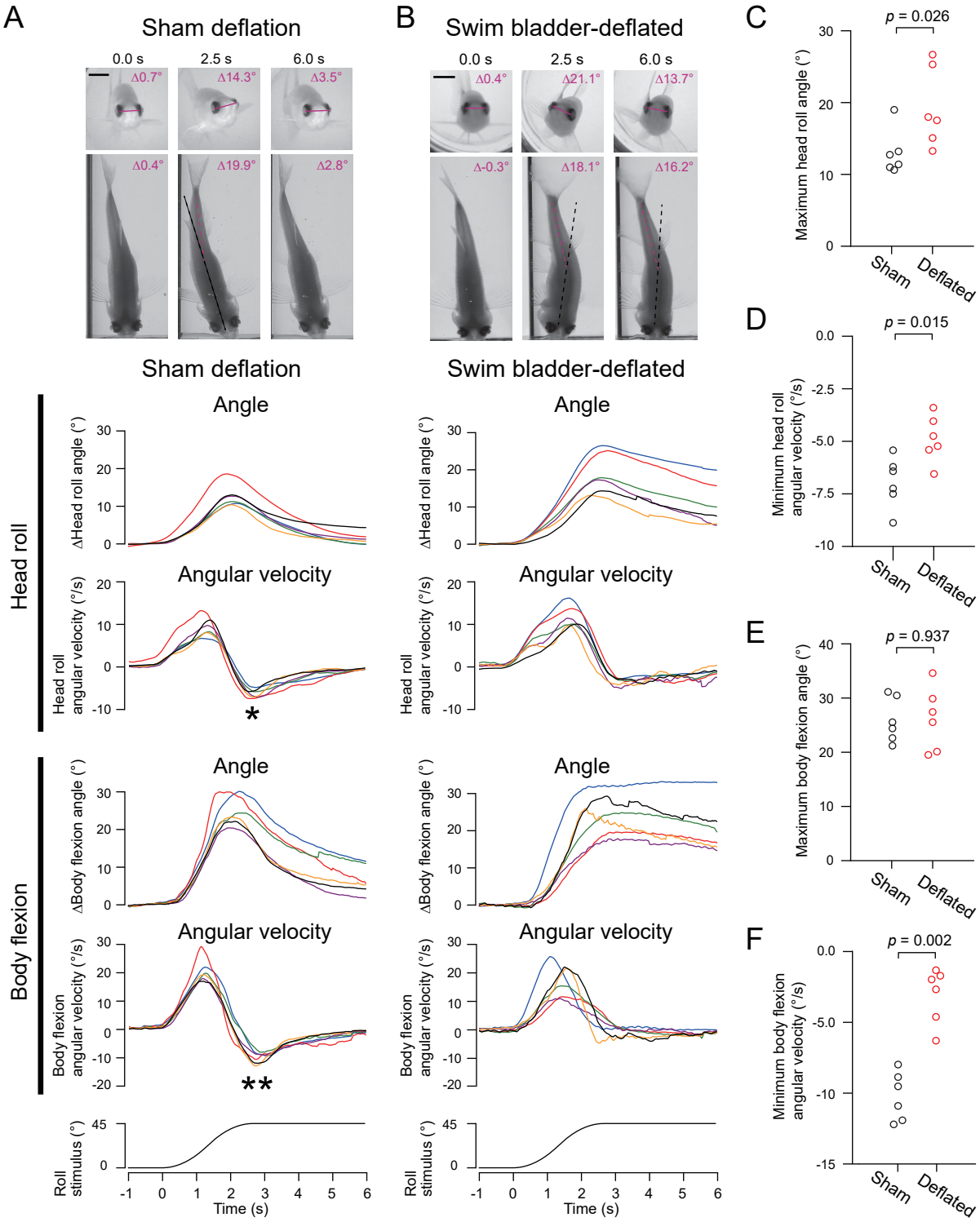
A
Sham deflation
0.0 s
2.5 s
6.0 s
Δ0.7°
Δ14.3°
Δ3.5°
Δ0.4°
Δ19.9°
Δ2.8°
B
Swim bladder-deflated
0.0 s
2.5 s
6.0 s
Δ0.4°
Δ21.1°
Δ13.7°
Δ-0.3°
Δ18.1°
Δ16.2°
Sham deflation
Swim bladder-deflated
Head roll
Angle
ΔHead roll angle (°)
Angular velocity
Head roll angular velocity (°/s)
*
Body flexion
Angle
ΔBody flexion angle (°)
Angular velocity
Body flexion angular velocity (°/s)
**
Roll stimulus (°)
Time (s)
C
p = 0.026
Maximum head roll angle (°)
Sham
Deflated
D
p = 0.015
Minimum head roll angular velocity (°/s)
E
p = 0.937
Maximum body flexion angle (°)
F
p = 0.002
Minimum body flexion angular velocity (°/s)

Figure 5

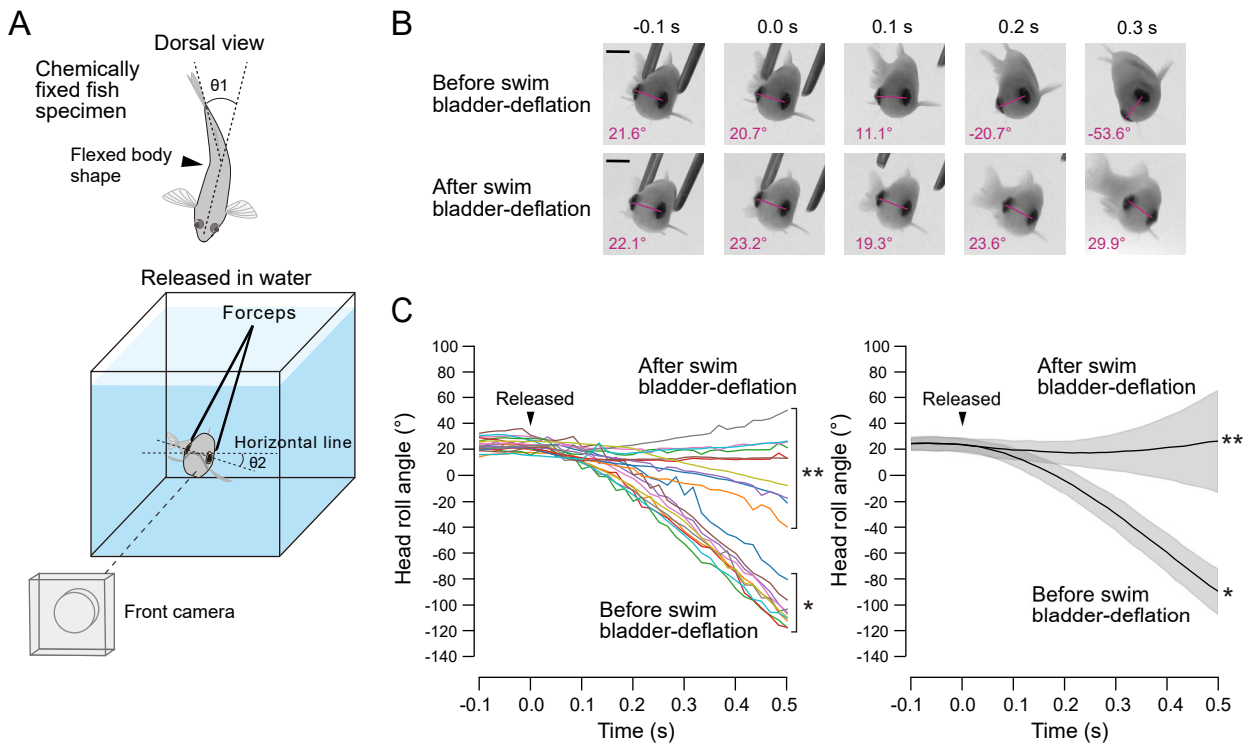
A
Dorsal view
Chemically fixed fish specimen
θ1
Flexed body shape
Released in water
Forceps
Horizontal line
θ2
Front camera
B
-0.1 s
0.0 s
0.1 s
0.2 s
0.3 s
Before swim bladder-deflation
21.6°
20.7°
11.1°
-20.7°
-53.6°
After swim bladder-deflation
22.1°
23.2°
19.3°
23.6°
29.9°
C
Head roll angle (°)
Released
After swim bladder-deflation
Before swim bladder-deflation
**
*
Time (s)